2022

Near-infrared spectroscopy estimation of combined skeletal muscle oxidative capacity and O2 diffusion capacity in humans

Andrea M. Pilotto

Alessandra Adami

Raffaele Mazzolari

Lorenza Brocca

Emanuela Crea

See next page for additional authors

Authors

Andrea M. Pilotto, Alessandra Adami, Raffaele Mazzolari, Lorenza Brocca, Emanuela Crea, Lucrezia Zuccarelli, Maria A. Pellegrino, Roberto Bottinelli, Bruno Grassi, Harry B. Rossiter, and Simone Porcelli

Near-infrared spectroscopy estimation of combined skeletal muscle oxidative capacity and O_2 diffusion capacity in humans

Pilotto AM[1,2], Adami A[3], Mazzolari R[2,4], Brocca L[2], Crea E[2], Zuccarelli L[1], Pellegrino MA[2,5], Bottinelli R[2,5], Grassi B[1], Rossiter HB[6] and Porcelli S[2,7]

[1] Department of Medicine, University of Udine, Udine, Italy

[2] Department of Molecular Medicine, University of Pavia, Pavia, Italy

[3] Department of Kinesiology, University of Rhode Island, Kingston, RI, USA

[4] Department of Physical Education and Sport, University of the Basque Country (UPV/EHU), Vitoria-Gasteiz, Spain

[5] Interdipartimental Centre for Biology and Sport Medicine, University of Pavia, Pavia, Italy

[6] Division of Respiratory and Critical Care Physiology and Medicine, The Lundquist Institute for Biomedical Innovation at Harbor–UCLA Medical Center, Torrance, CA, USA

[7] Institute of Biomedical Technologies, National Research Council, Milan, Italy

This is an Accepted Article that has been peer-reviewed and approved for publication in The Journal of Physiology, but has yet to undergo copy-editing and proof correction. Please cite this article as an 'Accepted Article'; doi: 10.1113/JP283267.

Corresponding author

Simone Porcelli, MD PhD

Assistant Professor in Human Physiology

Institute of Physiology

Department of Molecular Medicine

University of Pavia, Italy

Via Forlanini 6, 27100 Pavia - Italy

+39 0382987538

simone.porcelli@unipv.it

KEY POINTS SUMMARY

- We determined post-exercise recovery kinetics of quadriceps muscle oxygen uptake ($m\dot{V}O_2$) measured by near-infrared spectroscopy (NIRS) in humans under conditions of both non-limiting (HIGH) and limiting (LOW) O_2 availability, for comparison with biopsy variables.
- The $m\dot{V}O_2$ recovery rate constant in HIGH O_2 availability was hypothesized to reflect muscle oxidative capacity (k_{HIGH}); and the difference in k between HIGH and LOW O_2 availability (Δk) was hypothesized to reflect muscle O_2 diffusing capacity.
- k_{HIGH} was correlated with phosphorylating oxidative capacity of permeabilized muscle fiber bundles (r=0.80).
- Δk was negatively correlated with capillary density (r=-0.68) of biopsy samples.
- NIRS provides non-invasive means of assessing both muscle oxidative and oxygen diffusing capacity *in vivo*.

ABSTRACT

The final steps of the O_2 cascade during exercise depend on the product of the microvascular-to-intramyocyte PO_2 difference and muscle O_2 diffusing capacity (DmO_2). Non-invasive methods to determine DmO_2 in humans are currently unavailable. Muscle oxygen uptake ($m\dot{V}O_2$) recovery rate constant (k), measured by near-infrared spectroscopy (NIRS) using intermittent arterial occlusions, is associated with muscle oxidative capacity *in vivo*. We reasoned that k would be limited by DmO_2 when muscle oxygenation is low (k_{LOW}), and hypothesized that: i) k in well-oxygenated muscle (k_{HIGH}) is associated with maximal O_2 flux in fiber bundles; and ii) Δk (k_{HIGH}-k_{LOW}) is associated with capillary density (CD). Vastus lateralis k was measured in 12 participants using NIRS after moderate exercise. The timing and duration of arterial occlusions were manipulated to maintain tissue saturation index (TSI) within a 10% range either below (LOW) or above (HIGH) half-maximal desaturation, assessed during sustained arterial occlusion. Maximal O_2 flux in phosphorylating state was 37.7±10.6 $pmol \cdot s^{-1} \cdot mg^{-1}$ (~5.8 $ml \cdot min^{-1} \cdot 100g^{-1}$). CD ranged 348 to 586 mm^{-2}. k_{HIGH} was greater than k_{LOW} (3.15±0.45 vs 1.56±0.79 min^{-1}, $p<0.001$). Maximal O_2 flux was correlated with k_{HIGH} ($r=0.80$, $p=0.002$) but not k_{LOW} ($r=-0.10$, $p=0.755$). Δk ranged -0.26 to -2.55 min^{-1}, and correlated with CD ($r=-0.68$, $p=0.015$). $m\dot{V}O_2$ k reflects muscle oxidative capacity only in well-oxygenated muscle. Δk, the difference in k between well- and poorly-oxygenated muscle, was associated with CD, a mediator of DmO_2. Assessment of muscle k and Δk using NIRS provides a non-invasive window on muscle oxidative and O_2 diffusing capacity.

RUNNING TITLE: muscle oxidative and O_2 diffusing capacity by NIRS

KEYWORDS:

Recovery kinetics, skeletal muscle, mitochondria, capillary density, biopsy

INTRODUCTION

The primary source of ATP supply in skeletal muscle during endurance exercise is ADP phosphorylation coupled to the reduction of O_2 (Picard *et al.*, 2016). Two primary resistances, limiting the maximal conductance of O_2 from the atmosphere to the muscle mitochondrion, reside within the cardiovascular system (i.e., convective O_2 transport) and at the muscle capillary-myocyte interface (i.e., diffusive O_2 transport) (Wagner, 1992, 1995, 2000; Richardson *et al.*, 1995*a*).

The interaction of the maximum rate of convective O_2 transport and muscle O_2 diffusing capacity (DmO_2) determines the maximal muscle O_2 uptake ($m\dot{V}O_2$) (Roca *et al.*, 1992), the final steps of the O_2 cascade determining $m\dot{V}O_2$ depend on the product of the transmembrane PO_2 gradient (microvascular (mv) to intramyocyte (im) PO_2) and the muscle diffusing capacity for O_2 (DmO_2) (Fick's law of diffusion):

$$m\dot{V}O_2 = DmO_2 \times (PmvO_2 - PimO_2) \qquad \text{Eq. 1}$$

where ($PmvO_2 - PimO_2$) is strongly dependent on convective O_2 delivery and muscle O_2 demand (as a function of power output). This results in $PimO_2$ becoming essentially constant at ~1-5 mmHg during exercise above ~50% maximum O_2 uptake ($\dot{V}O_{2max}$) (Richardson *et al.*, 1995*b*; Clanton *et al.*, 2013). DmO_2, on the other hand, is a complex function of muscle capillarity, the surface area of apposition of red blood cells to capillary endothelium, red blood cell capillary transit time, haemoglobin volume, and the O_2 solubility properties within the diffusion pathway (Honig *et al.*, 1984; Groebe & Thews, 1986; Bebout *et al.*, 1993; Wagner, 1995; Poole *et al.*, 2020). Notwithstanding these confounding variables, DmO_2 is related to capillary density (CD; the number of capillaries per summed muscle fiber cross-sectional area) (Saltin & Gollnick, 1983; Hepple *et al.*, 2000; Poole *et al.*, 2020, 2021, 2022). The observed linear relationship between estimated $PmvO_2$ and $\dot{V}O_{2max}$ supports the concept that DmO_2 is a major limiting variable for $m\dot{V}O_{2max}$ in humans (Roca *et al.*, 1992; Richardson *et al.*, 1999). Methods to estimate DmO_2 in humans *in vivo* are complex and previous attempts on quadriceps muscle required invasive procedures with repeated exercise tests using breathing of gas mixtures containing high and low fractions of inspired O_2. Another approach, using non-invasive venous occlusion plethysmography to assess capillarity filtration (Brown *et al.*, 2001) provides an indirect estimation of limb capillarity, but is sensitive to changes in oncotic pressure, endothelial tight junctions and influenced by all tissues within the limb, not only muscle (Hunt *et al.*, 2013).

We sought to simplify assessment of DmO_2 in human quadriceps using a more muscle specific approach. We reasoned that, if we could make non-invasive measurements of $m\dot{V}O_2$ under two different ($PmvO_2 – PimO_2$) conditions (i.e. HIGH and LOW), we would be able to solve for DmO_2 by simultaneous subtraction of the two unknowns ($m\dot{V}O_2$ and $PmvO_2$, respectively) in Eq. 1, assuming, as in Roca et al. (1992), that $PimO_2$ is negligible. Near-infrared spectroscopy (NIRS) provides a relatively simple and non-invasive means to estimate muscle oxidative capacity (Grassi & Quaresima, 2016; Hamaoka & McCully, 2019). The recovery rate constant of $m\dot{V}O_2$ (k) established from the rate of decline in muscle tissue saturation index (TSI) under serial, intermittent, arterial occlusions (Hamaoka *et al.*, 1996; Motobe *et al.*, 2004; Ryan *et al.*, 2012; Adami *et al.*, 2017; Adami & Rossiter, 2018) shows good agreement with estimates of muscle oxidative capacity by other techniques e.g., phosphocreatine recovery time constant (r = 0.88 – 0.95) (Ryan *et al.*, 2013) or respiratory rates in fiber bundles (r = 0.61 – 0.74) (Ryan *et al.*, 2014).

We modified the NIRS-based assessment of $m\dot{V}O_2$ by manipulating the timing and duration of the intermittent arterial occlusions, thereby controlling the mean ($PmvO_2 – PimO_2$) at, separately, both HIGH (non-O_2 limiting) and LOW (O_2 limiting) values following moderate exercise. More specifically, we used k as proxy for $m\dot{V}O_2$ and TSI as a proxy of PmvO2. Although not without limitations, this approach led us to solve the Fick's law of diffusion as follows:

$$k = DmO_2 \times TSI$$

where PimO2 is considered negligible.

Then, we calculated k for both HIGH (k_{HIGH}) and low (k_{LOW}) TSI values and we compared the k values with variables obtained from biopsy taken from the same muscle location and individuals. We hypothesized that the recovery rate constant of $m\dot{V}O_2$ in high TSI conditions (k_{HIGH}) is associated with muscle oxidative capacity assessed using high resolution respirometry of permeabilized muscle fiber bundles.

Finally, we estimated DmO_2 from the difference in k values obtained in HIGH and LOW conditions ($\Delta k = k_{HIGH} - k_{LOW}$) and by calculating ΔTSI, according to the following equation:

$$\Delta k / \Delta TSI = DmO_2 \sim CD$$

We then tested the hypothesis that the difference in the recovery rate constant of $m\dot{V}O_2$ between HIGH and LOW TSI conditions (Δk) is associated with capillary density (CD) from biopsy histology.

MATERIALS AND METHODS

Subjects

Twelve moderately trained male (n = 7) and female (n = 5) adult participants (age 28 ± 5 yrs; weight 64.3 ± 10.2 kg; height 173 ± 7 cm) were recruited from the local community. All participants completed a health history questionnaire to ensure there was no presence of chronic disease. None of the participants took any medications known to alter metabolism. Participants were fully informed about the aims, methods, and risks, and gave their written informed consent prior to enrollment. All procedures were in accordance with the Declaration of Helsinki and the study was approved by the local ethics committee (Besta 64-19/07/2019).

Study Design

Participants visited the laboratory on four non-consecutive days over a 2-wk period (**Fig. 1**). They were instructed to abstain from strenuous physical activity for at least 24 h prior to each testing session (48 h for the biopsy trial). At visit 1, anthropometric measurements were taken, and an incremental cardiopulmonary exercise test to the limit of tolerance was administered on an electronically braked cycle ergometer (LC-6, Monark, Sweden) to determine $\dot{V}O_{2peak}$ and gas exchange threshold (GET). At visits 2 and 3, participants performed repeated muscle oxidative capacity tests within HIGH or LOW muscle oxygenation conditions (2 repeats at each visit), immediately after 5 min constant work-rate cycling at 80% GET (Zuccarelli *et al.*, 2020). At visit 4, approximately 100 mg of skeletal muscle was obtained from the *vastus lateralis* muscle by percutaneous conchotome muscle biopsy under local anesthesia (1% lidocaine) for muscle respirometry and morphology.

Incremental exercise

Power during step-incremental cycling was increased 10-15 W every minute, depending on the individual's fitness. Participants were instructed to maintain constant cadence at their preferred value (between 70 and 85 rpm). Intolerance was defined when participants could no longer maintain their chosen pedaling frequency despite verbal encouragement. Pulmonary gas exchange and ventilatory variables were determined breath-by-breath using a metabolic cart (Vyntus CPX, Vyaire Medical GmbH, Germany), which was calibrated following the manufacturer's instructions before each test. HR was recorded by using a chest band (HRM-Dual, Garmin, Kansas, USA), and rating of perceived exertion (RPE) was determined using Borg® 6–20 scale (Borg, 1982). At rest, and at 1, 3, and 5 min of recovery, 20 µL of capillary blood was obtained from a preheated earlobe for blood lactate concentration (Biosen C-line, EKF, Germany). Peak cardiopulmonary variables were measured from the highest 20 s mean values prior to intolerance. GET was determined by two independent investigators by using the modified "V-slope" method (Beaver *et al.*, 1986). The power at GET was estimated after accounting for the individual's $\dot{V}O_2$ mean response time (Whipp *et al.*, 1981).

Muscle Oxygen Uptake Recovery Rate Constant by NIRS

The $m\dot{V}O_2$ recovery *k* was measured using an approach modified from Zuccarelli et al. (Zuccarelli *et al.*, 2020). Oxygenation changes of the *vastus lateralis* were sampled at 10Hz by a wireless, portable, continuous-wave, spatially-resolved, NIRS device (PortaLite, Artinis, The Netherlands). Briefly, this device is equipped with three fiber optic bundles: NIR light is emitted from three optodes at two wavelengths (760 nm and 850 nm) and received from a fourth optode for transmission back to the data acquisition unit to determine the relative concentrations of deoxy- and oxy-genated heme groups contained in hemoglobin (Hb) and myoglobin (Mb). This method does not distinguish between the contributions of Hb and Mb to the NIRS signal, but Mb signal was assumed to be of minor impact compared to the contribution of Hb (Grassi & Quaresima, 2016). Relative concentrations of deoxy-(hemoglobin+myoglobin) (Δ[deoxy(Hb+Mb)]) and oxy-(hemoglobin+myoglobin) (Δ[oxy(Hb+Mb)] were measured in the tissues approximately 1.5 – 2 cm beneath the probe, with respect to an initial value obtained at rest before any procedure arbitrarily set equal to zero. From these measurements, relative changes in total hemoglobin and myoglobin (Δ[tot(Hb+Mb)] = Δ[oxy(Hb+Mb)] + Δ[deoxy(Hb+Mb)]) and the Hb difference (Δ[diff(Hb+Mb)] = Δ[oxy(Hb+Mb)] – Δ[deoxy(Hb+Mb)]) were calculated. In addition, the tissue saturation index (TSI, %) was measured using the spatially-resolved spectroscopy (SRS) approach (Ferrari *et al.*, 2004).

The skin at the NIRS probe site was shaved before the probe was placed longitudinally on the lower third of *vastus lateralis* muscle (~10 cm above the knee joint), and secured with a black patch and

elastic bandage. The location of the probe was marked using a skin marker to ensure the placement location was similar across all visits. The mean thickness of the skin and subcutaneous tissue at the NIRS probe site (7.8 ± 3.1 mm) was measured by skinfold caliper (Holtain Ltd, Crymych, UK). A 13 × 85 cm rapid-inflation pressure-cuff (SC12D, Hokanson, USA) was placed proximally on the same thigh and attached to an electronically-controlled rapid cuff-inflator (E20, Hokanson, USA).

While participants were seated on a cycle ergometer, baseline TSI and Δ[tot(Hb+Mb)] were measured over 2 min of rest. Subsequently, a prolonged arterial occlusion (300 mmHg) was performed until TSI plateaued (typically ~120 s). The cuff was instantly deflated and muscle reoxygenation was recorded until a steady-state was reached (typically ~3 min). This procedure identified the physiological normalization (PN) of TSI which was standardized to 0% at the deflection point (TSI min) and 100% at the maximum value reached during reperfusion (TSI max) (Adami *et al.*, 2017) (**Fig. 1**). Participants then cycled for 5 min at a target of 80% GET, followed by an immediate stop and 10-20 intermittent arterial occlusions at 300 mmHg. Duration and timing of the repeated occlusions were controlled by the investigator to maintain TSI in two different ranges: from 0 to 10% of PN (LOW) and from 50 to 60% of PN (HIGH), where the total amplitude of PN was used as 0-100% reference range (**Fig. 1**). The HIGH range was selected to ensure that occlusions were performed under well oxygenated conditions, and to avoid the reduction in PO_2 could limit $m\dot{V}O_2$ (i.e. maintaining TSI above 50% of the physiological normalization) (Haseler *et al.*, 2004, Adami & Rossiter, 2018). The LOW range was selected as the lowest boundary to evaluate $m\dot{V}O_2$ recovery k in poorly-oxygenated conditions, without overstepping the deflection point (i.e., where TSI during occlusions loses linearity). On the same day two repetitions of repeated occlusions protocol, separated by a resting period (typically ~5 min), were performed in a randomized order for both the LOW and HIGH experimental conditions.

The rate of muscle desaturation during each intermittent arterial occlusion (TSI, $\%\cdot s^{-1}$) was fitted to estimate the exponential $m\dot{V}O_2$ recovery or k, as previously described (Adami *et al.*, 2017) (**Fig. 2**). Data were quality-checked before curve fitting to remove invalid values or outliers i.e., low initial TSI values, or incomplete occlusions (Beever *et al.*, 2020). The test-retest variability of k was first assessed. Subsequently k within each condition (k_{HIGH} and k_{LOW}) was calculated from the mean of the two repeated measurements, and the difference between these conditions was calculated ($\Delta k = k_{HIGH.} - k_{LOW}$). Δ[tot(Hb+Mb)] above rest was measured during the arterial occlusions of both HIGH and LOW conditions.

Muscle Biopsy

Resting muscle biopsies were taken from the *vastus lateralis* muscle using a 130 mm (6") Weil-Blakesley rongeur (NDB-2, Fehling Instruments, GmbH&Co, Germany) under local anesthesia (1% lidocaine). After collection, muscle samples were cleaned of excess blood, fat, and connective tissue in ice-cold BioPS, a biopsy-preserving solution containing (in mM) 2.77 CaK_2EGTA, 7.23 K_2EGTA, 5.77 Na_2ATP, 6.56 $MgCl_2$, 20 taurine, 50 MES (2-(N-morpholino)ethanesulfonic acid), 15 Na_2phosphocreatine, 20 imidazole, and 0.5 dithiothreitol adjusted to pH 7.1 (Doerrier *et al.*, 2018). A portion of each muscle sample (~10-20 mg) was immediately placed in BioPS plus 10% (w/v) fatty acid free bovine serum albumin (BSA) and 30% (v/v) dimethyl sulfoxide (DMSO) and quickly frozen in liquid nitrogen; subsequently this portion was stored at -80°C for measurements of mitochondrial respiration within one month (Kuznetsov *et al.*, 2003). The remaining portion were fixed in OTC (Tissue-Tek, Sakura Finetek Europe, Zoeterwoude, The Netherlands) embedding medium, frozen in N_2-cooled isopentane and stored at -80°C for subsequent histology.

Preparation of Permeabilized Fibers

Fiber bundles were quickly thawed at room temperature by immersion in BioPS containing 2 $mg \cdot ml^{-1}$ BSA to remove any residual DMSO from the tissue (Kuznetsov *et al.*, 2003; Wüst *et al.*, 2012). Fibers were mechanically separated with pointed forceps in ice-cold BioPS under magnification (70×) (Stereomicroscope CRYSTAL-PRO, Konus-optical & sports systems, Italy). The plasma membrane was permeabilized by gentle agitation for 30 min at 4°C in 2 ml of BioPS containing 50 $\mu g \cdot ml^{-1}$ saponin, washed for 10 min in 2 ml of MiR06 (MiR05 + catalase 280 $IU \cdot ml^{-1}$) (in mM, unless specified) 0.5 EGTA, 3 $MgCl_2$, 60 potassium lactobionate, 20 taurine, 10 KH_2PO_4, 20 HEPES (4-(2-hydroxyethyl)piperazine-1-ethanesulfonic acid), 110 sucrose, and 1 $g \cdot L^{-1}$ BSA, essentially fatty acid–free (pH 7.1) (Doerrier *et al.*, 2018) and blotted prior to being weighed.

Mitochondrial Respiration

Mitochondrial respiration was measured in duplicate or triplicate, using 3-6 mg wet weight of muscle fibers, in 2ml of MiR06 at 37°C containing myosin II-ATPase inhibitor (25µM blebbistatin dissolved in DMSO 5mM stock) to inhibit contraction (Perry *et al.*, 2011) (Oxygraph-2k, Oroboros, Innsbruck, Austria). Chamber O_2 concentration was maintained between 250 and 450 $nmol \cdot ml^{-1}$ (average O_2 partial pressure 250 mmHg) to avoid O_2 limitation of respiration. Intermittent reoxygenation steps were performed during the experiments by injections of 1-3 µl of 0.3 mM H_2O_2, which was

instantaneously dismutated by catalase, already present in the medium, to O_2 and H_2O. Instruments were calibrated according to the manufacturer's instructions (Pesta & Gnaiger, 2012).

A substrate-uncoupler-inhibitor titration protocol was used (Salvadego *et al.*, 2016, 2018; Doerrier *et al.*, 2018) in the following order: glutamate (10 mM) and malate (4 mM) was added to assess LEAK respiration through complex I (CI_L). ADP (10 mM) was added to assess maximal oxidative phosphorylation (OXPHOS) capacity through CI (CI_P). Succinate (10 mM) was added to assess OXPHOS capacity through CI + complex II ($CI+II_P$). Cytochrome c (10 µM) added to test for outer mitochondrial membrane integrity. Stepwise additions of carbonyl cyanide-p trifluoromethoxyphenylhydrazone (FCCP) (0.5 – 1.5 µM) were used to measure electron transport system capacity through CI+II ($CI+II_E$). Inhibition of CI by rotenone (1 µM) determined electron transport system capacity through CII (CII_E), while addition of antimycin A (2.5 µM) was used to measure residual oxygen consumption, which was subtracted from all measurements. Results were expressed in $pmol \cdot s^{-1} \cdot mg^{-1}$ wet weight calculating mean values of duplicate analyses. At the conclusion of each experiment, muscle samples were removed from the chamber, immediately frozen in liquid nitrogen and then stored at -80°C until measurement of CS activity.

Citrate Synthase Activity

Muscle samples were thawed and underwent a motor-driven homogenization in a pre-cooled 1 mL glass-glass potter (Wheaton, USA). The muscle specimen was suspended 1:50 w/v in a homogenization buffer containing sucrose (250 mM), Tris (20 mM), KCl (40 mM) and EGTA (2 mM) with 1:50 v/v protease (P8340-Sigma) inhibitors. The specimen was homogenized in an ice-bath with 20 strokes at 500 rpm; before the last hit Triton X-100 (0.1% v/v) was added to the solution. After this, the sample was left in ice for 30 min. The homogenate was centrifuged at 14,000 g for 10 min. The supernatant was used to evaluate protein concentration according to the method of Lowry et al. (1951) (Lowry *et al.*, 1951). Protein extracts (5–10–15 µg) were added to each well of a 96-well-microplate along with 100 µl of 200 mM Tris, 20 µl of 1 mM 5, 5'-dithiobis-2-nitrobenzoate (DTNB), freshly prepared, 6 µl of 10mM acetyl-coenzyme A (Acetyl-Co-A) and mQ water to a final volume of 190 µl. A background ΔAbs, to detect any endogenous activity by acetylase enzymes, was recorded for 90 s with 10 s intervals at 412 nm at 25°C by an EnSpire 2300 Multilabel Reader (PerkinElmer). The ΔAbs was subtracted from the one given after the addition of 10 µl of 10 mM oxalacetic acid that started the reaction. All assays were performed at 25°C in triplicate on homogenates. Activity was expressed as $nmol \cdot min^{-1}$ (mU) per mg of protein. This protocol was modified from (Srere, 1969; Spinazzi *et al.*, 2012).

Cross-Sectional Area (CSA) Analysis

Muscle fiber CSA was determined from several transverse sections (10 μm thick) obtained from muscle samples and probed with anti-Dystrophin antibody. Fluorescence images were visualized with Olympus microscope (U-CMAD3). Fiber CSA was measured with Image J analysis software (NIH, Bethesda, MD, USA) and expressed in square micrometers. 125 to 150 fibers per sample were measured.

Capillarization

Several transverse 10 μm sections were obtained from muscle samples mounted in OTC. Sections were collected at – 20-22°C on the surface of a polarized glass slide. Cryosections were fixed with methanol in ice for 15 min, washed 3 times (5 min each) in PBS (NaCl 136mM, KCl 2mM, Na_2HPO_4 6mM, KH_2PO_4 1mM) at room temperature (RT) and incubated in 1%Triton-100x in PBS for 30 min (RT). Cryosections were then incubated with blocking reagents (4% BSA in 1% Triton X-100 in PBS + 5% Goat Serum) for 30 min (RT), raised with PBS (3 times of 5 min each) and probed with anti-CD31 (1:100 dilution, Abcam) overnight at 4°C. After 3 washes (5 min each) in PBS, cryosections were incubated with Alexa-Fluor 488 anti-mouse (1:200 dilution; Abcam) for 60 min at room temperature. Finally, the samples were probed with anti-Dystrophin (1:500 dilution, Abcam) for 60 min at room temperature and then with Alexa-Fluor 488 anti-rabbit (1:200 dilution; Abcam) for 60 min at room temperature. Fluorescence intensity was visualized with Olympus microscope (U-CMAD3). 125 to 150 fibers were measured in each sample. Capillary density was defined as total number of capillaries per cross-sectional area of the associated muscle fibers (Hoppeler *et al.*, 1981; Mathieu-Costello *et al.*, 1988, 1991, 1992; Hepple *et al.*, 2000).

Statistical Analysis

Results are mean ± SD. Normal distribution was verified with Shapiro–Wilk test, and paired Student's t-test was used to compare differences between two means. $p < 0.05$ was considered significant. To assess within-subject test–retest reliability, Pearson coefficient (r), coefficient of variation (CV) and intraclass correlation coefficient (ICC) were calculated for k measurements performed on different days. Correlation between respirometry variables and k was performed to compare *ex vivo* and *in vivo* estimates of muscle oxidative capacity. Correlation between CD and Δk was performed to examine

the validity of NIRS to estimate DmO_2. Correlation analyses were expressed as Pearson coefficient (r). Prism 8.0 (GraphPad) was used for data analysis.

RESULTS

Incremental Exercise

$\dot{V}O_{2peak}$ was 37.1 ± 8.0 ml·min^{-1}·kg^{-1} (range, 22.0 – 50.2 ml·min^{-1}·kg^{-1}) at 214 ± 52 W. Peak heart rate was 192 ± 9 beats·min^{-1}, approximately 102% of the age-predicted maximum value. RER was 1.28 ± 0.08; $[La]_b$ was 11.27 ± 2.24 mmol·l^{-1}, and RPE was 19 ± 1. GET was 1.73 ± 0.41 l·min^{-1} (69% of $\dot{V}O_{2peak}$), corresponding to 129 ± 34 W.

Muscle Oxygen Uptake Recovery Rate Constant by NIRS

A total of 48 m$\dot{V}O_2$ recovery kinetics assessments were performed (24 in each of HIGH and LOW conditions) after 5-min moderate intensity exercises (87 ± 26 W). Average $\dot{V}O_2$ from last 60 s of exercise was 1.43 ± 0.38 l·min^{-1} and RER was 0.95 ± 0.03. At the end of exercise RPE was 10 ± 2 and $[La]_b$ was 1.47 ± 0.39 mmol·l^{-1}. During last 20 s of cycling quadriceps TSI averaged 62.7 ± 3.9% (corresponding to 50.4 ± 6.4% of PN).

k_{HIGH} was 3.15 ± 0.45 min^{-1} and 2.79 ± 0.55 min^{-1} for the first and second repeat respectively (range 1.88 - 4.01 min^{-1}). k_{HIGH} was not different between repeats (p = 0.1057). k_{LOW} was 1.56 ± 0.79 min^{-1} and 1.53 ± 0.57 min^{-1} for first and second repeat, respectively (range 0.38 - 2.65 min^{-1}). k_{LOW} was not different between repeats (p = 0.9299). Coefficient of variation for repeated measurements was 26% and 12% for LOW and HIGH, respectively. In all participants and each repeat, k_{HIGH} was greater than k_{LOW} (both $p < 0.001$). The individual test-retest reliability of k_{HIGH} and k_{LOW}, assessed on different days, was good ($r = 0.67$, $p < 0.001$; ICC = 0.68, CV = 19%) (**Fig. 3**). Having established reproducibility, the mean k for each condition was calculated for comparison with biopsy variables. Mean k_{HIGH} was 2.97 ± 0.36 min^{-1} and mean k_{LOW} was 1.54 ± 0.55 min^{-1}. Δk ranged from 0.26 to 2.55 min^{-1} with a mean value of 1.42 ± 0.69 min^{-1}. Immediately before the first cycling exercise, Δ[tot(Hb+Mb)] was 3.14 ± 0.77 μM and increased to 9.57 ± 4.52 μM and 11.20 ± 4.05 μM during arterial occlusions in HIGH and LOW respectively. During arterial occlusions, Δ[tot(Hb+Mb)] was significantly greater than rest (p = 0.007 and p = 0.002 for HIGH and LOW, respectively).

Muscle Mitochondrial Respiration and Capillarization

Measurements of mitochondrial O_2 flux in permeabilized muscle fibers are shown in **Table 1**. Maximal O_2 flux in phosphorylating state (CI+II$_P$) was 37.7 ± 10.6 pmol·s^{-1}·mg^{-1} (corresponding to 5.8 ml·min^{-1}·100g^{-1}) and maximal uncoupled O_2 flux (CI+II$_E$) was 56.8 ± 19.8 pmol·s^{-1}·mg^{-1} (corresponding to 8.8 ml·min^{-1}·100g^{-1}). CS activity was 74.3 ± 50.9 mU·mg^{-1} protein.

Two typical images of CD capillary density measurement are shown in **Figure 4**. Mean fiber CSA, fiber number and capillary number in each sample were 5083 ± 73 μm^{-2}, 134 ± 47 and 311 ± 108, respectively. CD was 469 ± 73 mm^{-2}, ranging from 348 to 586 mm^{-2} among individuals.

Correlations

k_{HIGH} was correlated with CI+II$_P$ ($r = 0.80$, $p < 0.01$) and CI+II$_E$ ($r = 0.81$, $p < 0.01$). k_{LOW} was not correlated with either CI+II$_P$ or CI+II$_E$ ($r = -0.10$ and $r = -0.11$, respectively) (**Fig 5A-B**). Δk was significantly correlated with capillary density ($r = -0.68$, $p = 0.015$) (**Fig. 5C**).

DISCUSSION

This study tested the hypotheses that m$\dot{V}O_2$ k is associated with muscle oxidative capacity only in high TSI conditions and that the difference in m$\dot{V}O_2$ k between well-oxygenated and poorly-oxygenated muscle provides insight into DmO_2. Our data confirmed previous findings (Ryan *et al.*, 2014) that, in well-oxygenated tissue, m$\dot{V}O_2$ recovery rate constant measured by NIRS, k_{HIGH}, is correlated with maximal muscle O_2 flux in fiber bundles. Additionally, we showed for the first time that this relationship did not hold when tissue oxygenation was reduced below 50% of the physiological normalization; and, k_{LOW} was not associated with any variable describing muscle O_2 flux in fiber bundles. This finding is consistent with Fick's law in that m$\dot{V}O_2$ becomes increasingly dependent on DmO_2 as microvascular-to-myocyte PO_2 difference is reduced (see Eq. 1). From this, we demonstrated that Δk, the difference between k_{HIGH} and k_{LOW}, was associated with capillary density ~~C:F~~ in biopsy samples of the same tissue, a primary structural determinant of DmO_2. Thus, the NIRS-derived response measured under conditions of both well-oxygenated and poorly-oxygenated skeletal muscle provided a non-invasive means of assessing both muscle oxidative capacity and muscle diffusing capacity *in vivo*. The application of this NIRS protocol may be of great interest for the study of skeletal muscle oxidative and diffusing capacities in response to exercise training or in disease states (e.g., heart failure, chronic obstructive pulmonary disease, myopathies).

NIRS and muscle oxidative capacity

In health, skeletal muscle oxidative capacity is strongly correlated with whole-body aerobic capacity and exercise performance (Holloszy, 1967; Hoppeler *et al.*, 1985; Hood *et al.*, 2011). Moreover, muscle oxidative capacity and mitochondrial function are impaired in conditions of physical inactivity (Buso *et al.*, 2019; Zuccarelli *et al.*, 2021), aging (Layec *et al.*, 2013) and chronic disease, such as obesity (Menshikova *et al.*, 2005; Lazzer *et al.*, 2013), diabetes (Joseph *et al.*, 2012) myopathy (Grassi *et al.*, 2019, 2020), pulmonary obstructive disease (Adami *et al.*, 2017, 2020), and neuromuscular disease (Breuer *et al.*, 2013). Traditionally, muscle oxidative capacity has been studied using *ex vivo* approaches involving muscle biopsy samples and measurement of enzyme activity, or mitochondrial respiratory capacity in isolated mitochondrial preparations and permeabilized muscle fibers (Chance & Williams, 1955; Holloszy, 1967; Gnaiger, 2009; Brand & Nicholls, 2011; Perry *et al.*, 2013). For a long time, *in vivo* approaches were limited to ^{31}P nuclear magnetic resonance spectroscopy (^{31}P-MRS) to measure the recovery rate of phosphocreatine (PCr) after exercise, which is associated with maximal O_2 flux in muscle (Kemp *et al.*, 1993; Blei *et al.*, 1993; Kent & Fitzgerald, 2016). Over the past decade, however, NIRS coupled with intermittent arterial occlusions, has proven a valuable tool to assess the $m\dot{V}O_2$ recovery rate constant, *k*, which is directly associated with muscle oxidative capacity (Hamaoka *et al.*, 1996; Motobe *et al.*, 2004; Ryan *et al.*, 2012; Grassi & Quaresima, 2016; Adami *et al.*, 2017; Adami & Rossiter, 2018; Hamaoka & McCully, 2019). The estimation of muscle oxidative capacity using NIRS has been already examined in upper and lower limb muscles and in both healthy subjects and patients affected by chronic diseases (Meyer, 1988; Erickson *et al.*, 2013, 2015; Ryan *et al.*, 2013, 2014; Harp *et al.*, 2016; Adami *et al.*, 2017; Willingham & McCully, 2017). However, muscle oxidative capacity estimation by NIRS relies on two main assumptions (Adami & Rossiter, 2018; Chung *et al.*, 2018): i) muscle contractions are sufficient to maximally activate mitochondrial oxidative enzymes, and ii) O_2 concentration at skeletal muscle level is not a limiting factor to oxidative phosphorylation. Regarding the first point, it has been demonstrated that the first-order relationship between PCr dynamics and ATP production by oxidative phosphorylation is valid only when mitochondrial oxidative enzymes are maximal activated. Additionally, experiments on isolated single frog muscle fibers show that maximal activation of mitochondrial enzymes may not be achieved when muscle stimulation (or contraction frequency) is too low (Wüst *et al.*, 2013). For this reason, we used 5 min of moderate intensity cycling to stimulate OXPHOS and activate a wide range of regulated enzymes within the mitochondrial matrix, with the goal to reach a high, ideally, maximal mitochondrial activation. Our data for k_{HIGH} show a good correlation with maximal O_2 flux in biopsy samples (either phosphorylating or uncoupled), consistent with the findings of others. These data confirm that NIRS provides a reasonable non-invasive estimate of muscle oxidative capacity when the tissue is well-oxygenated.

The second assumption, that O_2 concentration is not limiting in the NIRS test, has received relatively less attention. Because $m\dot{V}O_2$ depends in part on the O_2 pressure difference between the microvasculature and the inner mitochondrial membrane in the myocyte to facilitate O_2 diffusion, it stands to reason that reducing $PmvO_2$ could reduce O_2 flux and limit $m\dot{V}O_2$ *k*. This suggestion was confirmed previously by the reduction in $m\dot{V}O_{2max}$ and PCr recovery rate constant under conditions of reduced $PmvO_2$ imposed by breathing hypoxic gas mixtures (Haseler *et al.*, 1999, 2004; Richardson *et al.*, 1999). By reducing ($PmvO_2$ – $PimO_2$) in hypoxia, $m\dot{V}O_2$ becomes increasingly dependent on DmO_2 (Eq. 1). Despite this, no study to date investigated whether NIRS-derived $m\dot{V}O_2$ *k* estimation is affected by changes in O_2 availability. We investigated the reliability and validity of NIRS-derived $m\dot{V}O_2$ *k* to reflect muscle oxidative capacity under conditions of well- and poorly-oxygenated muscle. As expected, k_{HIGH} was associated with maximal O_2 flux in fiber bundles performed in a hyperoxic environment (i.e. in non-limiting O_2 availability), when TSI was maintained above 50% of PN (r = 0.80 to 0.81; **Fig 5A**) and showed good reproducibility (test-retest r = 0.67, ICC = 0.68, **Fig. 3**). The regression coefficient between methods was very similar to that observed by Ryan et al. (2014) (Ryan *et al.*, 2014). However, our data also show that this association was lost (r = -0.11 to -0.10) when the arterial occlusion protocol was experimentally manipulated to hold TSI between 0-10% PN. In the k_{LOW} condition, good test-retest reproducibility was maintained, but the association with maximal O_2 flux by tissue respirometry was absent (**Fig. 5B**).

The two NIRS tests assessed the same muscle region in tests applied a few minutes apart, therefore differences between k_{HIGH} and k_{LOW} could not reasonably reflect structural or functional properties in the skeletal muscle mitochondria. Rather, the difference reflects the increasing importance of DmO_2 in k_{LOW}, when ($PmvO_2$ - $PimO_2$) was reduced by experimental manipulation of the occlusion protocol. Thus, $m\dot{V}O_2$ *k* is only valid method to estimate muscle oxidative capacity when assessed as k_{HIGH} i.e., above 50% PN (Adami & Rossiter, 2018).

NIRS and muscle O_2 diffusion

As previously described, $m\dot{V}O_2$ is dependent on the interplay between both convective and diffusive transport (Roca *et al.*, 1992). In our protocol, we estimated muscle oxidative capacity from the TSI slope during repeated arterial occlusions, which minimizes the effects of O_2 delivery on the estimation of muscle oxidative capacity. Moreover, we effectively manipulated arterial occlusions such that the sum of ($PmvO_2$ - $PimO_2$) was either large or small, in the HIGH and LOW conditions respectively. In

these conditions, convective O_2 transport may have an influence on our surrogate measure of DmO_2 by modifying capillary Hb volume, RBC transit time, or RBCs immediately adjacent to active muscle fibers during the reperfusion phase between two occlusions. However, the absence of differences in Δ[tot(Hb+Mb)] between HIGH and LOW supports the notion that, under these strictly controlled experimental conditions, convective O_2 transport did not influence $m\dot{V}O_2$ *k*.

By measuring $m\dot{V}O_2$ under these two conditions we could simultaneously solve by elimination for DmO_2 (Eq. 1). Using NIRS the absolute value of ($PmvO_2$ - $PimO_2$) is unknown; rather the ranges of TSI used reflected two relative oxygenation values (i.e., HIGH and LOW). Also, absolute values of $m\dot{V}O_2$ are not precisely known using NIRS, although they may be estimated assuming values for tissue [Hb+Mb] (among other assumptions). Nevertheless, the NIRS-based protocol we used allows for relative measurement of $m\dot{V}O_2$ and ($PmvO_2$ - $PimO_2$), such that solving Eq. 1 for a relative estimate of DmO_2 is possible. We used the *k* value for $m\dot{V}O_2$, rather than $m\dot{V}O_2$ itself, because as demonstrated k_{HIGH} reflects muscle oxidative capacity and because the kinetics $m\dot{V}O_2$ are ~~agnostic~~ unrelated to absolute measurements (thereby reducing potential variability introduced by comparing absolute $m\dot{V}O_2$ values from NIRS). Assessment of DmO_2 was performed by capillary density and the finding that Δ*k* was correlated with CD (**Fig. 5C**) supports the validity of NIRS-based protocol to estimate DmO_2.

Although CD ~~C:F~~ does not assess length and diameter of vessels, the measurement of capillary density in a muscle cross section may provide information to understand the O_2 diffusing capacity of skeletal muscle (Saltin & Gollnick, 1983; Hepple *et al.*, 2000; Poole *et al.*, 2020, 2021, 2022). Our CD values ranged from 348 to 586 mm^{-2}, in line with published data (Poole *et al.*, 2020). On the other hand, Δ*k* ranged more widely from 0.26 to 2.55 min^{-1}. This is presumably because Δ*k* is also influenced by muscle oxidative capacity, therefore changes in Δ*k* under fixed TSI conditions may vary more widely than capillary structure alone. Nevertheless, the finding of a significant association between Δ*k* and CD may allow a valid non-invasive estimation of CD *in vivo*.

The ability to measure O_2 dynamics in microvessels in human skeletal muscles is currently beyond reach (Koga *et al.*, 2014; Lundby & Montero, 2015). Previous studies have attempted this by measuring structural components related to the path through plasma and capillary wall to the cytoplasm (e.g. capillary density) or calculating the ratio of $m\dot{V}O_2$ and O_2 pressure gradient between microvessels and mitochondria using the method developed by Wagner-and colleagues (Roca *et al.*,

1989, 1992; Richardson *et al.*, 1999; Hepple *et al.*, 2000). Although these elegant experiments were fundamental to move forward knowledge in the field, they do not fully account for the physiological mechanisms of *in vivo* regulation and reduce a complex diffusion process to a few key variables (Hepple *et al.*, 2000).

A step towards a more physiological approach was used by Brown et al. (Brown *et al.*, 2001). In endurance and resistance trained athletes, Brown et al. estimated capillary filtration capacity with plethysmography during small incremental steps in venous occlusion pressure. They found an association between filtration capacity and muscle capillarity, consistent with a relationship between capillary filtration and capillary surface area (Brown *et al.*, 2001; Hunt *et al.*, 2013). In our study we used NIRS to follow the flux of O_2 rather than fluid within the capillary-to-myofiber. In addition, NIRS is able to estimate changes in Δ[tot(Hb+Mb)] within the microvasculature, such that our NIRS-based method likely more closely reflects apposition of red-blood cells with capillary endothelium and therefore the O_2 diffusion pathway. The action of repeated occlusions has the effect of increasing Δ[tot(Hb+Mb)] in the microvasculature (~10 μM in Δ[tot(Hb+Mb)] from rest which should account for an increase in hematocrit of ~18%, leading to a total hematocrit of 33%), thereby generating a diffusional surface area that may be closer to *in vivo* condition when DmO_2 is maximized i.e., high longitudinal capillary recruitment at approach exercise at maximal aerobic capacity. That NIRS measures the oxygenation of all [Hb+Mb] within the field of view, may therefore, be a more valid reflection the final steps in O_2 cascade than structural properties of the capillaries alone. However, as yet undeveloped, more advanced techniques are needed to test this hypothesis.

The correlation coefficients of k with muscle oxidative capacity and Δk with CD were relatively small when compared with correlations for clinical techniques (Hanneman, 2008). However, the Pearson correlation coefficient resulting in our study ($r = 0.80$ and $r = -0.68$, respectively) was similar with other validation studies comparing *in vivo* methods with *ex vivo* approaches using NIRS ($r = 0.61 – 0.74$) (Ryan *et al.*, 2014). While NIRS and biopsy were taken from the same muscle region, the volumes assayed by each of these techniques are different (~2-3 cm^3 and ~1 mm^3, respectively). In addition, the structural and functional assessments differ between NIRS and biopsy. Unlike NIRS, maximal O_2 flux in fiber bundles in respirometry is assessed using supraphysiologic concentrations of substrates, including O_2, and reflects all fibers in the sample. Maximal O_2 flux based on NIRS signals derive from only those fibers that were active during the exercise, and therefore may be biased towards low order fibers (slow, oxidative). As discussed, CD is a structural contributor to DmO_2, but may not reflect to the true capacity for O_2 diffusion in tissue with variable capillary content of red blood cells. Therefore, variability between methods is expected, with the NIRS potentially having the

advantage that it assays a larger muscle volume than the biopsy, and assays under physiologic conditions *in vivo*.

CONCLUSIONS

In summary, we report reliability and accuracy of NIRS measurements of $m\dot{V}O_2$ during intermittent arterial occlusions protocols to estimate muscle oxidative capacity and muscle DmO_2 *in vivo*. The $m\dot{V}O_2$ recovery rate constant, *k*, was a reasonable and reliable method to assess muscle oxidative capacity only when assessed in well-oxygenated quadriceps muscle (>50% of TSI physiological normalization). Experimental manipulation of TSI through timing and duration of intermittent arterial occlusions provided a new variable, Δ*k*, which was the difference in *k* between well-oxygenated and poorly-oxygenated experimental conditions. As hypothesized, we found that Δ*k* was associated with CD, a structural determinant of DmO_2. Therefore, the NIRS-based protocol we describe represents a cost-effective and non-invasive means of assessing both muscle oxidative capacity and muscle O_2 diffusive capacity *in vivo*.

DATA AVAILABILITY STATEMENT

All relevant data are presented as individual data points in the figures. Data not presented with individual data points are available from the corresponding author upon request.

ACKNOWLEDGEMENTS

The authors would like to acknowledge the participants who joined the project and graduate students Andrea Alberti and Andrea Colombo for their help during data recording.

DISCLOSURES

Simone Porcelli was supported by a grant from Sports Medicine Italian Federation (FMSI01092021). Alessandra Adami is supported by a grant from NIH (R01HL151452). Harry Rossiter is supported by grants from NIH (R01HL151452, R01HL153460, P50HD098593, R01DK122767, P2CHD086851), the Tobacco Related Disease Research Program (T31IP1666), and the University of California, Office of the President. He reports consulting fees from Omniox Inc., and is involved in contracted clinical research with Boehringer Ingelheim, GlaxoSmithKline, Novartis, AstraZeneca, Astellas, United Therapeutics, Genentech and Regeneron. He is a visiting Professor at the University of Leeds, UK.

REFERENCES

Adami A, Cao R, Porszasz J, Casaburi R & Rossiter HB (2017). Reproducibility of NIRS assessment of muscle oxidative capacity in smokers with and without COPD. *Respir Physiol Neurobiol* **235,** 18–26.

Adami A, Corvino RB, Calmelat RA, Porszasz J, Casaburi R & Rossiter HB (2020). Muscle Oxidative Capacity Is Reduced in Both Upper and Lower Limbs in COPD. *Med Sci Sports Exerc* **52,** 2061–2068.

Adami A & Rossiter HB (2018). Principles, insights, and potential pitfalls of the noninvasive determination of muscle oxidative capacity by near-infrared spectroscopy. *J Appl Physiol* **124,** 245–248.

Beaver WL, Wasserman K & Whipp BJ (1986). A new method for detecting anaerobic threshold by gas exchange. *J Appl Physiol* **60,** 2020–2027.

Bebout DE, Hogan MC, Hempleman SC & Wagner PD (1993). Effects of training and immobilization on VO2 and DO2 in dog gastrocnemius muscle in situ. *J Appl Physiol* **74,** 1697–1703.

Beever AT, Tripp TR, Zhang J & MacInnis MJ (2020). NIRS-derived skeletal muscle oxidative capacity is correlated with aerobic fitness and independent of sex. *J Appl Physiol* **129,** 558–568.

Blei ML, Conley KE, Odderson IR, Esselman PC & Kushmerick MJ (1993). Individual variation in contractile cost and recovery in a human skeletal muscle. *Proc Natl Acad Sci U S A* **90,** 7396–7400.

Borg G (1982). Ratings of Perceived Exertion and Heart Rates During Short-Term Cycle Exercise and Their Use in a New Cycling Strength Test. *Int J Sports Med* **3,** 153–158.

Brand MD & Nicholls DG (2011). Assessing mitochondrial dysfunction in cells. *Biochem J* **435,** 297–312.

Breuer ME, Koopman WJ, Koene S, Nooteboom M, Rodenburg RJ, Willems PH & Smeitink JAM (2013). The role of mitochondrial OXPHOS dysfunction in the development of neurologic diseases. *Neurobiol Dis* **51,** 27–34.

Brown MD, Jeal S, Bryant J & Gamble J (2001). Modifications of microvascular filtration capacity in human limbs by training and electrical stimulation. *Acta Physiol Scand* **173,** 359–368.

Buso A, Comelli M, Picco R, Isola M, Magnesa B, Pišot R, Rittweger J, Salvadego D, Šimunič B, Grassi B & Mavelli I (2019). Mitochondrial adaptations in elderly and young men skeletal

muscle following 2 weeks of bed rest and rehabilitation. *Front Physiol*; DOI: 10.3389/FPHYS.2019.00474/PDF.

Chance B & Williams GR (1955). Respiratory enzymes in oxidative phosphorylation. IV. The respiratory chain. *J Biol Chem* **217,** 429–438.

Chung S et al. (2018). Commentaries on Viewpoint: Principles, insights, and potential pitfalls of the noninvasive determination of muscle oxidative capacity by near-infrared spectroscopy. *J Appl Physiol* **124,** 254–255.

Clanton TL, Hogan MC & Gladden LB (2013). Regulation of cellular gas exchange, oxygen sensing, and metabolic control. *Compr Physiol* **3,** 1135–1190.

Doerrier C, Garcia-Souza LF, Krumschnabel G, Wohlfarter Y, Mészáros AT & Gnaiger E (2018). High-Resolution FluoRespirometry and OXPHOS Protocols for Human Cells, Permeabilized Fibers from Small Biopsies of Muscle, and Isolated Mitochondria. *Methods Mol Biol* **1782,** 31–70.

Erickson ML, Ryan TE, Young HJ & McCully KK (2013). Near-infrared assessments of skeletal muscle oxidative capacity in persons with spinal cord injury. *Eur J Appl Physiol* **113,** 2275–2283.

Erickson ML, Seigler N, Mckie KT, Mccully KK & Harris RA (2015). Skeletal muscle oxidative capacity in patients with cystic fibrosis. *Exp Physiol* **100,** 545–552.

Ferrari M, Mottola L & Quaresima V (2004). Principles, techniques, and limitations of near infrared spectroscopy. *Can J Appl Physiol* **29,** 463–487.

Gnaiger E (2009). Capacity of oxidative phosphorylation in human skeletal muscle New perspectives of mitochondrial physiology. *Int J Biochem Cell Biol* **41,** 1837–1845.

Grassi B, Porcelli S & Marzorati M (2019). Translational Medicine: Exercise Physiology Applied to Metabolic Myopathies. *Med Sci Sports Exerc* **51,** 2183–2192.

Grassi B, Porcelli S & Marzorati M (2020). Metabolic Myopathies: “Human Knockout” Models and Translational Medicine. *Front Physiol*; DOI: 10.3389/FPHYS.2020.00350/PDF.

Grassi B & Quaresima V (2016). Near-infrared spectroscopy and skeletal muscle oxidative function in vivo in health and disease: a review from an exercise physiology perspective. *J Biomed Opt* **21,** 091313.

Groebe K & Thews G (1986). Theoretical analysis of oxygen supply to contracted skeletal muscle.

Adv Exp Med Biol **200,** 495–514.

Hamaoka T, Iwane H, Shimomitsu T, Katsumura T, Murase N, Nishio S, Osada T, Kurosawa Y & Chance B (1996). Noninvasive measures of oxidative metabolism on working human muscles by near-infrared spectroscopy. *J Appl Physiol* **81,** 1410–1417.

Hamaoka T & McCully KK (2019). Review of early development of near-infrared spectroscopy and recent advancement of studies on muscle oxygenation and oxidative metabolism. *J Physiol Sci* **69,** 799–811.

Hanneman SK (2008). Design, analysis, and interpretation of method-comparison studies. *AACN Adv Crit Care* **19,** 223–234.

Harp MA, McCully KK, Moldavskiy M & Backus D (2016). Skeletal muscle mitochondrial capacity in people with multiple sclerosis. *Mult Scler J - Exp Transl Clin*; DOI: 10.1177/2055217316678020.

Haseler LJ, Hogan MC & Richardson RS (1999). Skeletal muscle phosphocreatine recovery in exercise-trained humans is dependent on O2 availability. *J Appl Physiol* **86,** 2013–2018.

Haseler LJ, Lin AP & Richardson RS (2004). Skeletal muscle oxidative metabolism in sedentary humans: 31P-MRS assessment of O2 supply and demand limitations. *J Appl Physiol* **97,** 1077–1081.

Hepple RT, Hogan MC, Stary C, Bebout DE, Mathieu-Costello O & Wagner PD (2000). Structural basis of muscle O(2) diffusing capacity: evidence from muscle function in situ. *J Appl Physiol* **88,** 560–566.

Holloszy JO (1967). Biochemical Adaptations in Muscle: Effects of exercise on mitochondrial oxygen uptake and respiratory enzyme activity in skeletal muscle. *J Biol Chem* **242,** 2278–2282.

Honig CR, Gayeski TE, Federspiel W, Clark A & Clark P (1984). Muscle O2 gradients from hemoglobin to cytochrome: new concepts, new complexities. *Adv Exp Med Biol* **169,** 23–38.

Hood DA, Uguccioni G, Vainshtein A & D'souza D (2011). Mechanisms of exercise-induced mitochondrial biogenesis in skeletal muscle: implications for health and disease. *Compr Physiol* **1,** 1119–1134.

Hoppeler H, Howald H, Conley K, Lindstedt SL, Claassen H, Vock P & Weibel ER (1985). Endurance training in humans: aerobic capacity and structure of skeletal muscle. *J Appl Physiol* **59,** 320–327.

Hoppeler H, Mathieu O, Weibel ER, Krauer R, Lindstedt SL & Taylor CR (1981). Design of the mammalian respiratory system. VIII Capillaries in skeletal muscles. *Respir Physiol* **44,** 129–150.

Hunt JEA, Galea D, Tufft G, Bunce D & Ferguson RA (2013). Time course of regional vascular adaptations to low load resistance training with blood flow restriction. *J Appl Physiol* **115,** 403–411.

Joseph AM, Joanisse DR, Baillot RG & Hood DA (2012). Mitochondrial dysregulation in the pathogenesis of diabetes: potential for mitochondrial biogenesis-mediated interventions. *Exp Diabetes Res*; DOI: 10.1155/2012/642038.

Kemp GJ, Taylor DJ & Radda GK (1993). Control of phosphocreatine resynthesis during recovery from exercise in human skeletal muscle. *NMR Biomed* **6,** 66–72.

Kent JA & Fitzgerald LF (2016). In vivo mitochondrial function in aging skeletal muscle: capacity, flux, and patterns of use. *J Appl Physiol* **121,** 996–1003.

Koga S, Rossiter HB, Heinonen I, Musch TI & Poole DC (2014). Dynamic heterogeneity of exercising muscle blood flow and O2 utilization. *Med Sci Sports Exerc* **46,** 860–876.

Kuznetsov A V., Kunz WS, Saks V, Usson Y, Mazat JP, Letellier T, Gellerich FN & Margreiter R (2003). Cryopreservation of mitochondria and mitochondrial function in cardiac and skeletal muscle fibers. *Anal Biochem* **319,** 296–303.

Larsen S, Nielsen J, Hansen CN, Nielsen LB, Wibrand F, Stride N, Schroder HD, Boushel R, Helge JW, Dela F & Hey-Mogensen M (2012). Biomarkers of mitochondrial content in skeletal muscle of healthy young human subjects. *J Physiol* **590,** 3349–3360.

Layec G, Haseler LJ & Richardson RS (2013). Reduced muscle oxidative capacity is independent of O2 availability in elderly people. *Age (Dordr)* **35,** 1183–1192.

Lazzer S, Salvadego D, Porcelli S, Rejc E, Agosti F, Sartorio A & Grassi B (2013). Skeletal muscle oxygen uptake in obese patients: functional evaluation by knee-extension exercise. *Eur J Appl Physiol* **113,** 2125–2132.

Lowry OH, Rosebrough NJ, Farr AL & Randall RJ (1951). Protein measurement with the Folin phenol reagent. *J Biol Chem* **193,** 265–275.

Lundby C & Montero D (2015). CrossTalk opposing view: Diffusion limitation of O2 from microvessels into muscle does not contribute to the limitation of V̇O2 max. *J Physiol* **593,** 3759–3761.

Mathieu-Costello O, Ellis CG, Potter RF, MacDonald IC & Groom AC (1991). Muscle capillary-to-fiber perimeter ratio: morphometry. *Am J Physiol*; DOI: 10.1152/AJPHEART.1991.261.5.H1617.

Mathieu-Costello O, Potter RF, Ellis CG & Groom AC (1988). Capillary configuration and fiber shortening in muscles of the rat hindlimb: correlation between corrosion casts and stereological measurements. *Microvasc Res* **36,** 40–55.

Mathieu-Costello O, Suarez RK & Hochachka PW (1992). Capillary-to-fiber geometry and mitochondrial density in hummingbird flight muscle. *Respir Physiol* **89,** 113–132.

Menshikova E V., Ritov VB, Toledo FGS, Ferrell RE, Goodpaster BH & Kelley DE (2005). Effects of weight loss and physical activity on skeletal muscle mitochondrial function in obesity. *Am J Physiol Endocrinol Metab*; DOI: 10.1152/AJPENDO.00322.2004.

Meyer RA (1988). A linear model of muscle respiration explains monoexponential phosphocreatine changes. *Am J Physiol*; DOI: 10.1152/AJPCELL.1988.254.4.C548.

Motobe M, Murase N, Osada T, Homma T, Ueda C, Nagasawa T, Kitahara A, Ichimura S, Kurosawa Y, Katsumura T, Hoshika A & Hamaoka T (2004). Noninvasive monitoring of deterioration in skeletal muscle function with forearm cast immobilization and the prevention of deterioration. *Dyn Med* **3,** 1–11.

Perry CGR, Kane DA, Lanza IR & Neufer PD (2013). Methods for assessing mitochondrial function in diabetes. *Diabetes* **62,** 1041–1053.

Perry CGR, Kane DA, Lin C Te, Kozy R, Cathey BL, Lark DS, Kane CL, Brophy PM, Gavin TP, Anderson EJ & Neufer PD (2011). Inhibiting myosin-ATPase reveals a dynamic range of mitochondrial respiratory control in skeletal muscle. *Biochem J* **437,** 215–222.

Pesta D & Gnaiger E (2012). High-resolution respirometry: OXPHOS protocols for human cells and permeabilized fibers from small biopsies of human muscle. *Methods Mol Biol* **810,** 25–58.

Picard M, Wallace DC & Burelle Y (2016). The rise of mitochondria in medicine. *Mitochondrion* **30,** 105–116.

Poole DC, Kano Y, Koga S & Musch TI (2021). August Krogh: Muscle capillary function and oxygen delivery. *Comp Biochem Physiol A Mol Integr Physiol*; DOI: 10.1016/J.CBPA.2020.110852.

Poole DC, Musch TI & Colburn TD (2022). Oxygen flux from capillary to mitochondria: integration of contemporary discoveries. *Eur J Appl Physiol* **122,** 7–28.

Poole DC, Pittman RN, Musch TI & Østergaard L (2020). August Krogh's theory of muscle microvascular control and oxygen delivery: a paradigm shift based on new data. *J Physiol* **598,** 4473–4507.

Richardson RS, Grassi B, Gavin TP, Haseler LJ, Tagore K, Roca J & Wagner PD (1999). Evidence of O2 supply-dependent V̇O(2max) in the exercise-trained human quadriceps. *J Appl Physiol* **86,** 1048–1053.

Richardson RS, Knight DR, Poole DC, Kurdak SS, Hogan MC, Grassi B & Wagner PD (1995*a*). Determinants of maximal exercise VO2 during single leg knee-extensor exercise in humans. *Am J Physiol*; DOI: 10.1152/AJPHEART.1995.268.4.H1453.

Richardson RS, Noyszewski EA, Kendrick KF, Leigh JS & Wagner PD (1995*b*). Myoglobin O2 desaturation during exercise. Evidence of limited O2 transport. *J Clin Invest* **96,** 1916–1926.

Roca J, Agusti AGN, Alonso A, Poole DC, Viegas C, Barbera JA, Rodriguez-Roisin R, Ferrer A & Wagner PD (1992). Effects of training on muscle O2 transport at VO2max. *J Appl Physiol* **73,** 1067–1076.

Roca J, Hogan MC, Story D, Bebout DE, Haab P, Gonzalez R, Ueno O & Wagner PD (1989). Evidence for tissue diffusion limitation of VO2max in normal humans. *J Appl Physiol* **67,** 291–299.

Ryan TE, Brophy P, Lin C Te, Hickner RC & Neufer PD (2014). Assessment of in vivo skeletal muscle mitochondrial respiratory capacity in humans by near-infrared spectroscopy: a comparison with in situ measurements. *J Physiol* **592,** 3231–3241.

Ryan TE, Erickson ML, Brizendine JT, Young HJ & McCully KK (2012). Noninvasive evaluation of skeletal muscle mitochondrial capacity with near-infrared spectroscopy: correcting for blood volume changes. *J Appl Physiol* **113,** 175–183.

Ryan TE, Southern WM, Reynolds MA & McCully KK (2013). A cross-validation of near-infrared spectroscopy measurements of skeletal muscle oxidative capacity with phosphorus magnetic resonance spectroscopy. *J Appl Physiol* **115,** 1757–1766.

Saltin B & Gollnick PD (1983). Skeletal Muscle Adaptability: Significance for Metabolism and Performance. *Compr Physiol*555–631.

Salvadego D, Keramidas ME, Brocca L, Domenis R, Mavelli I, Rittweger J, Eiken O, Mekjavic IB & Grassi B (2016). Separate and combined effects of a 10-d exposure to hypoxia and inactivity on oxidative function in vivo and mitochondrial respiration ex vivo in humans. *J Appl Physiol* **121,**

154–163.

Salvadego D, Keramidas ME, Kölegård R, Brocca L, Lazzer S, Mavelli I, Rittweger J, Eiken O, Mekjavic IB & Grassi B (2018). PlanHab*: hypoxia does not worsen the impairment of skeletal muscle oxidative function induced by bed rest alone. *J Physiol* **596,** 3341–3355.

Spinazzi M, Casarin A, Pertegato V, Salviati L & Angelini C (2012). Assessment of mitochondrial respiratory chain enzymatic activities on tissues and cultured cells. *Nat Protoc* **7,** 1235–1246.

Srere PA (1969). Citrate synthase: EC 4.1.3.7. Citrate oxaloacetate-lyase (CoA-acetylating)]. *Methods Enzymol* **13,** 3–11.

Wagner PD (1992). Gas exchange and peripheral diffusion limitation. *Med Sci Sports Exerc* **24,** 54–58.

Wagner PD (1995). Limitations of oxygen transport to the cell Background and present knowledge. *Intensive Care Med* **21,** 391–398.

Wagner PD (2000). Diffusive resistance to O2 transport in muscle. *Acta Physiol Scand* **168,** 609–614.

Whipp BJ, Davis JA, Torres F & Wasserman K (1981). A test to determine parameters of aerobic function during exercise. *J Appl Physiol* **50,** 217–221.

Willingham TB & McCully KK (2017). In vivo assessment of mitochondrial dysfunction in clinical populations using near-infrared spectroscopy. *Front Physiol*; DOI: 10.3389/FPHYS.2017.00689/PDF.

Wüst RCI, van der Laarse WJ & Rossiter HB (2013). On-off asymmetries in oxygen consumption kinetics of single Xenopus laevis skeletal muscle fibres suggest higher-order control. *J Physiol* **591,** 731–744.

Wüst RCI, Myers DS, Stones R, Benoist D, Robinson PA, Boyle JP, Peers C, White E & Rossiter HB (2012). Regional skeletal muscle remodeling and mitochondrial dysfunction in right ventricular heart failure. *Am J Physiol Heart Circ Physiol*; DOI: 10.1152/AJPHEART.00653.2011.

Zuccarelli L, Baldassarre G, Magnesa B, Degano C, Comelli M, Gasparini M, Manferdelli G, Marzorati M, Mavelli I, Pilotto A, Porcelli S, Rasica L, Šimunič B, Pišot R, Narici M & Grassi B (2021). Peripheral impairments of oxidative metabolism after a 10-day bed rest are upstream of mitochondrial respiration. *J Physiol* **599,** 4813–4829.

Zuccarelli L, Do Nascimento Salvador PC, Del Torto A, Fiorentino R & Grassi B (2020). Skeletal muscle V̇o 2 kinetics by the NIRS repeated occlusions method during the recovery from cycle ergometer exercise. *J Appl Physiol* **128,** 534–544.

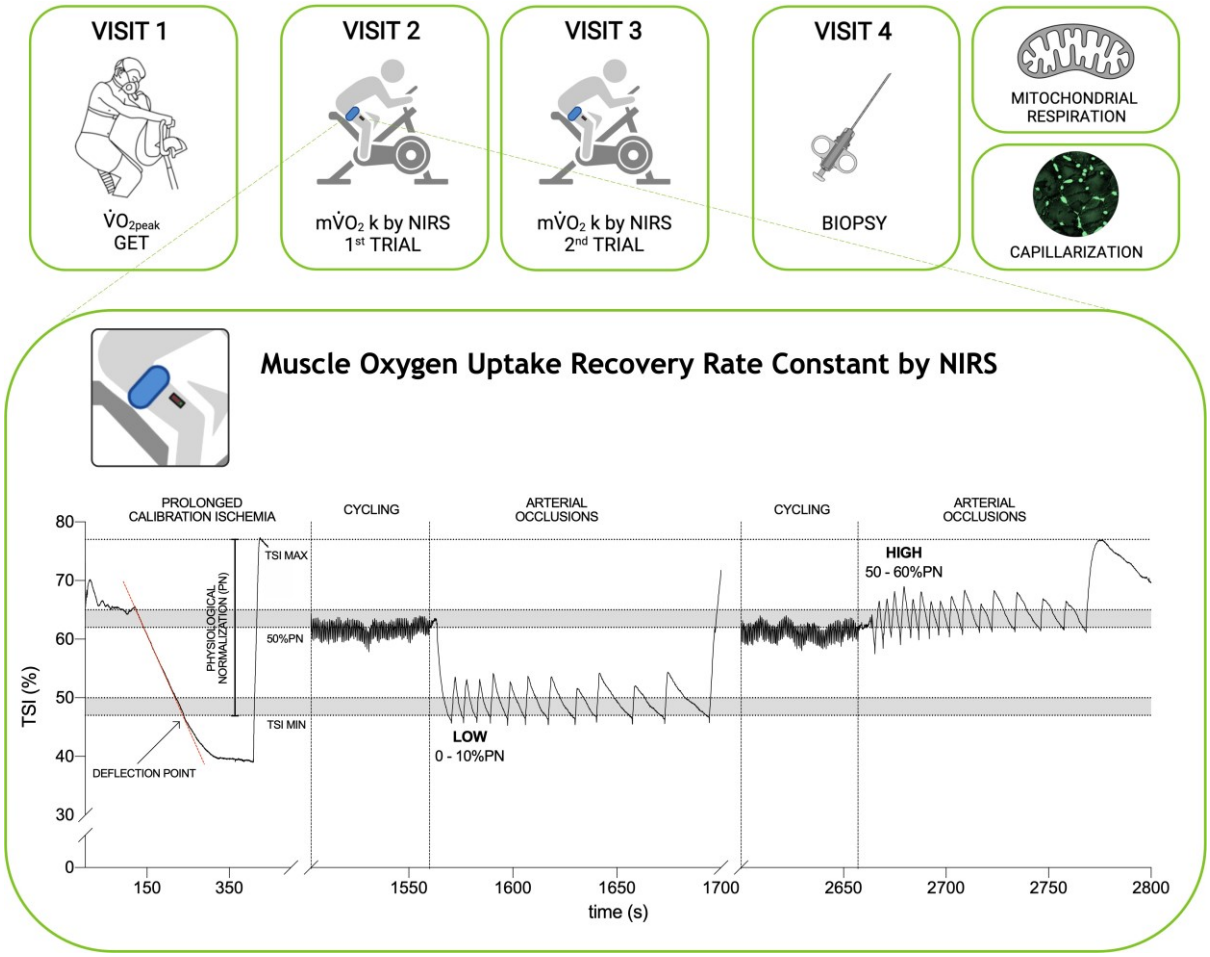

Figure 1. Study design and muscle recovery rate constant (*k*) protocol by NIRS

Participants visited the laboratory on 4 occasions. Visit 1 was used to determine peak oxygen uptake ($\dot{V}O_{2peak}$) and gas exchange threshold (GET). Visits 2 and 3 were used to determine the physiological normalization (PN) of quadriceps TSI following sustained arterial occlusion, and the muscle $\dot{V}O_2$ recovery rate constant (*k*) in well-oxygenated (HIGH) and poorly-oxygenated (LOW) conditions. Two *k* measurements were performed at each visit. To measure *k*, participants initially cycled for 5 min at 80% GET, followed immediately by 10-20 intermittent arterial occlusions (300 mmHg). The duration and timing of repeated occlusions were modulated in order to maintain TSI in two different ranges: from 0 to 10% of PN (LOW) and from 50 to 60% of PN (HIGH). A muscle biopsy was obtained in visit 4.

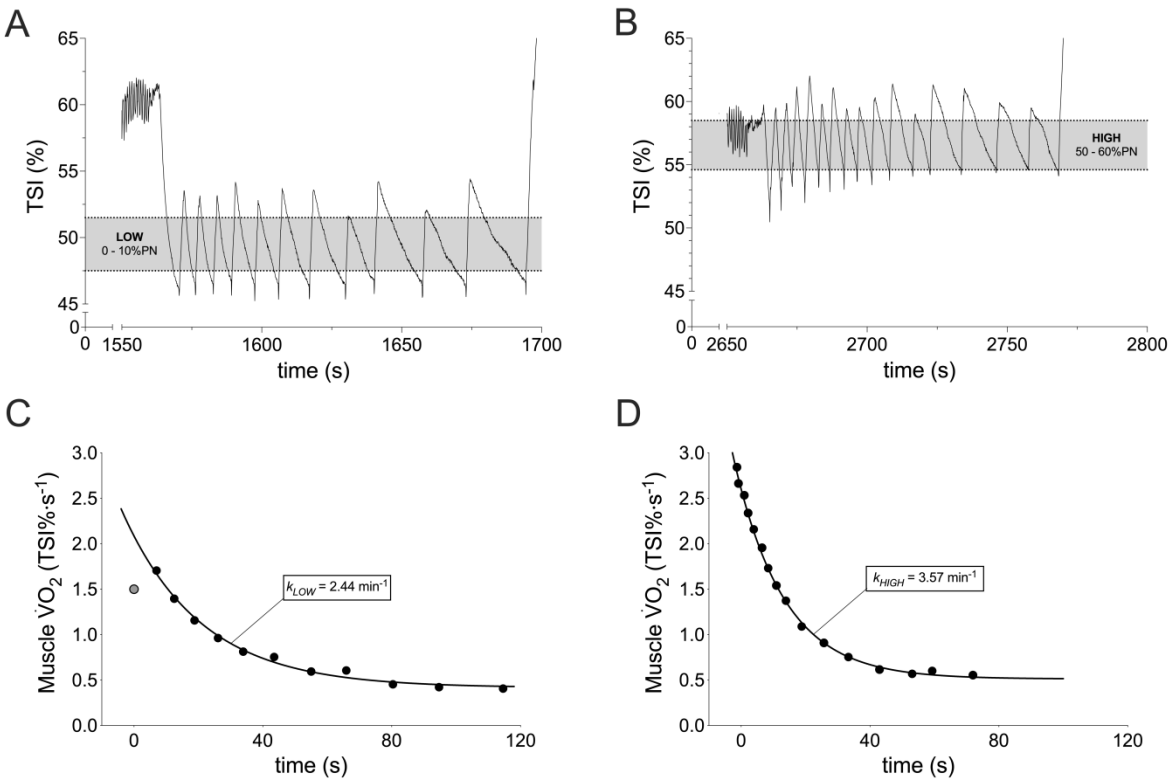

Figure 2. Representative tissue saturation index (TSI) responses during repeated arterial occlusions of the quadriceps following moderate exercise in LOW and HIGH conditions.

Representative muscle TSI profiles and $m\dot{V}O_2$ recovery kinetics during intermittent arterial occlusions following 5 min moderate intensity cycling. **A)** TSI profile in poorly-oxygenated (LOW; TSI = 0-10% of physiological normalization) condition. **B)** TSI profile in well-oxygenated (TSI = 50-60% of physiological normalization) condition. **C)** $m\dot{V}O_2$ recovery and exponential fit (black line) for calculation of k_{LOW}. **D)** $m\dot{V}O_2$ recovery and exponential fit (black line) for calculation of k_{HIGH}. Grey point represents outlier, excluded from the analysis (see methods). *k* is the recovery rate constant. n=1.

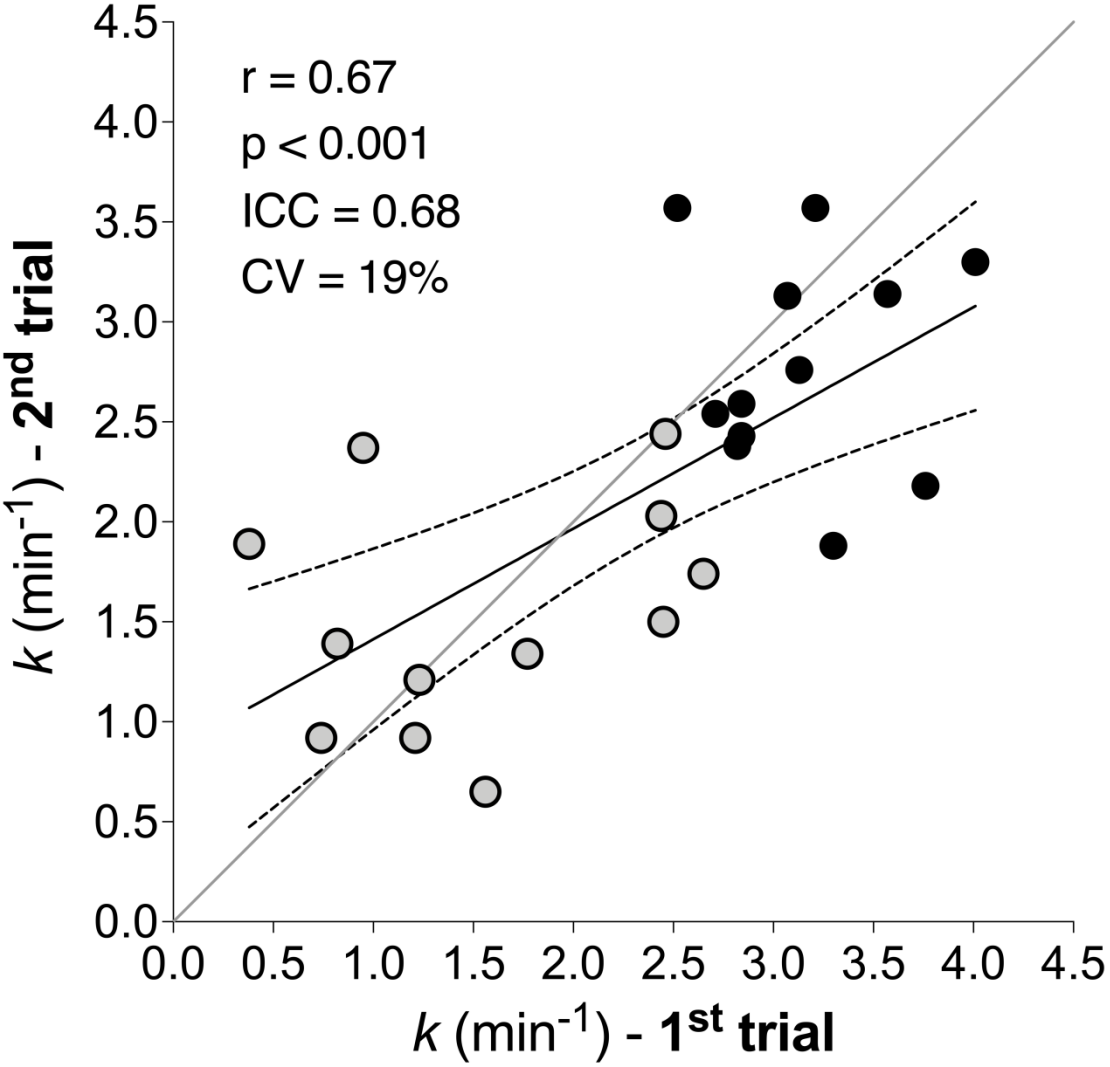

Figure 3. Individual test-retest reliability of muscle oxidative capacity by NIRS

The individual test-retest reliability of recovery rate constant (*k)* assessed by NIRS in different days during both HIGH (black circles) and LOW (grey circles) on 12 participants. Straight line represents linear regression curve and dashed line represent 95% confidence intervals. Grey line represents identity. Circles represent *k* values obtained during first and second trial.

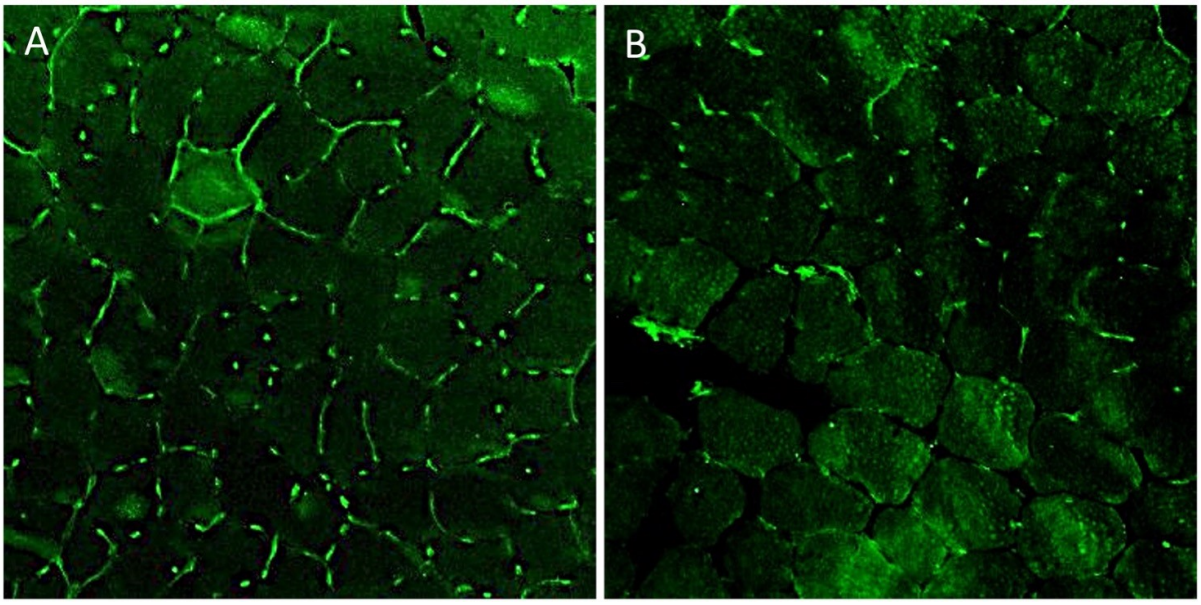

Figure 4. Muscle capillarization from two participants.

Immunofluorescent identification of capillaries in cross sections of *vastus lateralis* from two participants. **A)** Participant with the highest capillary density. **B)** Participant with the lowest capillary density. After immunostaining using anti-CD31, capillaries appear green. (n=2).

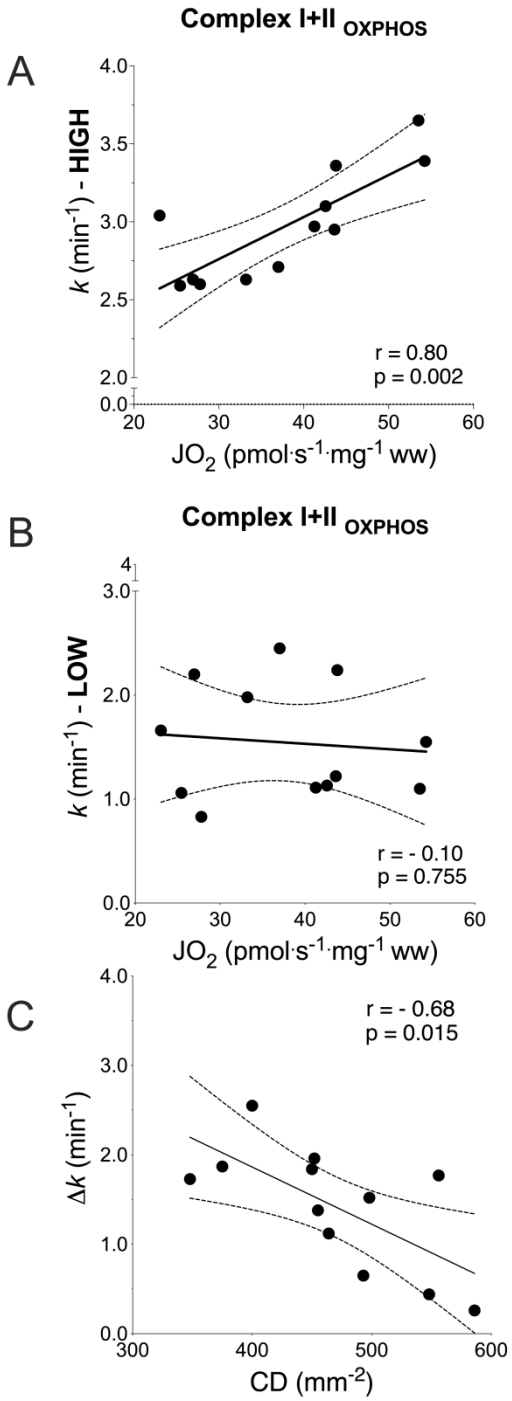

Figure 5. Association between *in vivo* (NIRS) and *ex vivo* (biospy) estimation of (A-B) skeletal muscle OXPHOS capacity and (C) skeletal muscle capillary density.

Correlation between muscle oxidative phosphorylation capacity by high-resolution respirometry and recovery rate constant by NIRS measured in HIGH (**A**) and LOW (**B**) conditions. **C)** Correlation between Δk (= k_{HIGH} - k_{LOW}) by NIRS and capillary density (CD) from biopsy. Δk is lower in participants with a greater muscle capillarization. Linear regression (solid) 95% confidence intervals (dash). n=12.

Table 1. Mitochondrial O_2 flux in permeabilized muscle fibers

Mass specific ($pmol \cdot s^{-1} \cdot mg^{-1}$)	CI_L	CI_P	$CI+II_P$	$CI+II_E$	CII_E
Mean ± SD	6.0 ± 3.2	14.6 ± 5.8	37.7 ± 10.6	56.8 ± 19.8	45.3 ± 14.8
Min	0.0	4.5	23.0	33.6	29.1
Max	11.3	23.9	54.3	99.9	76.6

CI_L, leak respiration through CI; CI_P, maximum coupled mitochondrial respiration through CI; $CI+II_P$, maximum coupled mitochondrial respiration through CI+II; $CI+II_E$, maximum noncoupled mitochondrial respiration through CI+II; CII_E, maximum noncoupled mitochondrial respiration through CII. Mitochondrial respiration was measured in duplicate or triplicate, n=12.

Andrea M. Pilotto is a Research Assistant at the Department of Molecular Medicine, University of Pavia, and a PhD student in Biomedical Sciences and Biotechnology at the Department of Medicine, University of Udine. He completed MS Degree in Sport Science at the University of Milan. His research focuses on molecular, metabolic and physiological mechanisms underlying adaptations to exercise, with particular emphasis on the effects of exercise training on mitochondrial adaptations.

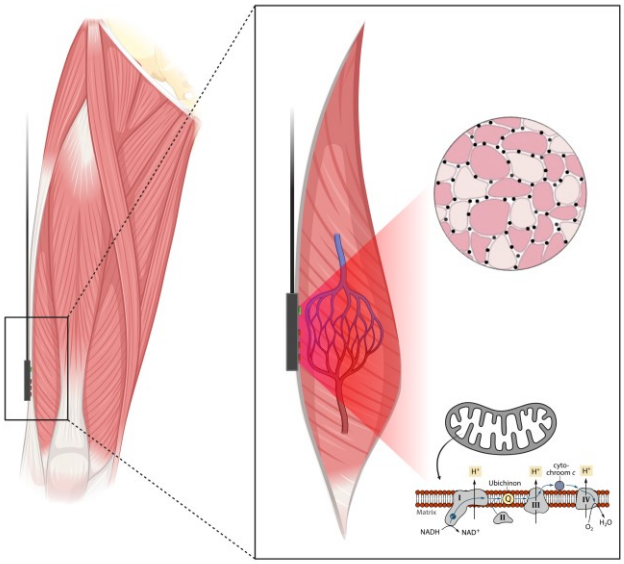

Abstract figure As for Larsen et al, please delete the reference from the list. GRAPHICAL ABSTRACT LEGEND NIRS probe was positioned on vastus lateralis muscle and used to assess both muscle oxidative and oxygen diffusing capacity in vivo by intermittent arterial occlusions. Timing and duration of each occlusion were manipulated to maintain tissue saturation index (TSI) within a 10percentage range either below (LOW) or above (HIGH) half-maximal desaturation. Recovery rate constant (k) of muscle oxygen consumption (mV O2) obtained by NIRS was correlated to phosphorylating oxidative capacity of permeabilized muscle fiber bundles. Changes in recovery rate constant (k) were correlated to capillary density calculated from cross-section of muscle samples obtained by immunofluorescence